KSCE Journal of Civil Engineering (2016) 20(1):261-272
DOI 10.1007/s12205-015-0538-2

Structural Engineering
pISSN 1226-7988, eISSN 1976-3808
www.springer.com/12205

Seismic Analysis of Roller Compacted Concrete (RCC) Dams Considering Effect of Sizes and Shapes of Galleries

Khaled Ghaedi*, Mohammed Jameel, Zainah Ibrahim***, and P. Khanzaei******

Received September 12, 2014/Revised November 18, 2014/Accepted December 15, 2014/Published Online March 18, 2015

Abstract

This paper compares the analysis of a Roller Compacted Concrete (RCC) dam with and without galleries under seismic loading. The effects of different sizes and shapes (circle, octagon and square) of gallery have also seen in the analysis. For this purpose, two-dimensional (2D) Finite Element Model (FEM) is used for nonlinear dynamic analysis by means of finite element software, ABAQUS. In addition, Concrete Damaged Plasticity (CDP) model is also implemented to inspect the tensile damage of the dam during earthquake excitation. Kinta RCC dam of Malaysia is considered as a case study in analysis. From the seismic analysis, it was found that by increasing the size of openings, stress is developed around the galleries. As a result, the gallery with circle shape is more appropriate for the dam in comparison to gallery with square and octagon shapes. From crack propagation analysis and displacement response, it was also found that the gallery with circle shape behaves better than the gallery with square and octagon shaped.

Keywords: *RCC dam, Concrete Damaged Plasticity (CDP), gallery, nonlinear dynamic analysis, hydrodynamic pressure*

1. Introduction

The estimation of the seismic response of RCC dams under earthquake excitation is a complex problem and several factors play the roles in this field, such as interaction effects amongst dam, reservoir and foundation. On the other hand, effects of openings inside the dam body and the presence of tension centralization around the openings cause tensile damage inside and outside of body of dams which take away the water into the core of the dam (Jin *et al*., 2005). In addition, the hydrodynamic pressure due to the impounded water and dam deformation under earthquake excitations interact with each other and the significance of hydrodynamic pressure effect on dam behavior subjected to earthquake has been recognized. Thus, the effect of water level under earthquake response has to consider in the nonlinear dynamic analysis (Akkose *et al*., 2008; Perumalswami and Kar, 1973). (Bower, 2010; Aguíñiga *et al.*, 2010; Ahmad, 2007; Akkose *et al.*, 2008).

Skrikerud and Bachmann (1986) studied the crack propagation of the Koyna gravity dam by using single crack model. The results showed that there was a relationship between aggregate forces and surface of openings. Ayari (1990) investigated the fracture mechanics based model and discrete crack closure model for Koyna dam under dynamic loading in transient condition.

Guanglun *et al.* (2000) proposed a mathematical model based on the nonlinear crack band theory to investigate the dynamic fracture behavior of gravity dams in two-dimensional FEM. Also, they presented the finite element remesh for the front cracks via shifting the element edge couples of cracks in direction of the tensile stresses. The smeared crack model was used to inspect the nonlinear dynamic response of dams considering reservoir water effect under earthquake excitations (Arash Mazloumi *et al.*, 2012; Ayari, 1990). Zhu and Pekau (2007) employed and adopted the Incremental Displacement Constraint Equations (IDCE) model along the crack to consider the behavior of dynamic contact states in the cracks. The damping model of IDCE was validated in dynamic contact conditions for flexible and rigid bodies. The obtained results revealed very attractive occurrences such as peak rocking direction, jumping and large damping effect of multi cracks on the peak residual sliding. Researchers have also discussed about seismic behavior of dams by implementation of two-dimensional finite element modeling, such as Calayir and Karaton (2005), Yuchuan *et al.* (2009), Akköse and Simsek (2010), Jiang and Du (2012), Mazloumi *et al*. (2012), Zhang *et al.* (2013), Paggi et al

*Research Assistant, Dept. of Civil Engineering, University of Malaya, 50603, Malaysia; Hormoz Beton Firm, Bandar Abbas City, Iran (Corresponding Author, E-mail: khaledqhaedi@ yahoo.com)
**Senior Lecturer, Dept. of Civil Engineering, University of Malaya, 50603, Malaysia (E-mail: jameel@um.edu.my)
***Senior Lecturer, Dept. of Civil Engineering, University of Malaya, 50603, Malaysia (E-mail: zainah@um.edu.my)
****Ph.D. Student, Candidate at Institute for Infrastructure Engineering, University of Western Sydney, Australia (E-mail: Parvin.khanzaei@gmail.com)

(2013) and others. However, the effects of opening on dams have been neglected in the above studies.

The researchers have carried out seismic analyses of concrete gravity dams, but the effect of galleries is ignored. Shirkande and Dawari (2011), however have considered three models of galleries on a typical concrete gravity dam body. The study was about the effect of size and shape variations of huge galleries without considering the hydrodynamic pressure effect of the reservoir water on the dam. Currently there is a need to pay more attentions to gallery effects in the analysis of Roller Compacted Concrete (RCC) dams under dynamic loadings, including the hydrodynamic pressure. The construction of concrete gravity dams and RCC dams are highly dissimilar. In this research, the galleries effect on tensile damage is inspected on RCC dams, when their shape and size is changed. The hydrodynamic pressure effect of reservoir water on dam is also taken into account. The effects of hydrodynamic pressure and galleries on RCC dams under earthquake ground motions will also help in assessing the actual nonlinear dynamic behavior and tensile damage response of the dam. This paper attempts to focus on the gallery's shape and size effects on RCC dams by considering of the opening inside the dam body under earthquake excitation. Meantime, dam-reservoir interaction with fixed foundation is implemented, therefore, through this study the dam is fixed at its base level. No sediment effect has been established for model. Kinta RCC dam which is located in Malaysia with 81.8 m height and 63.5 m width is chosen as a case study.

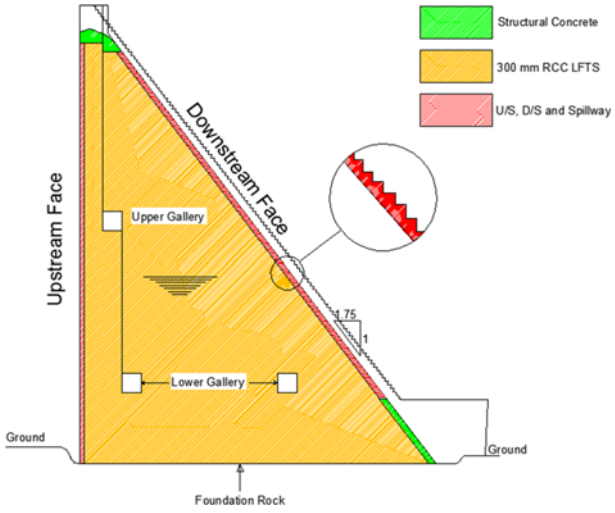

Fig. 1. Typical Cross Section of the Dam and Location of Galleries

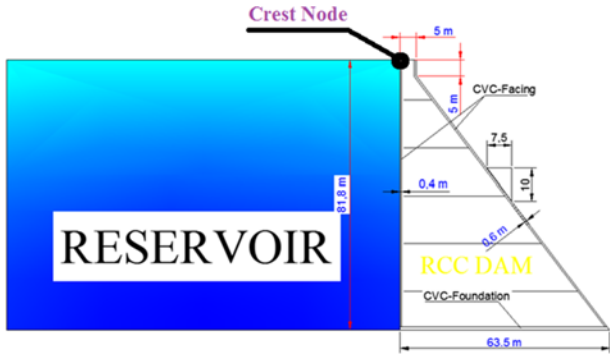

Fig. 2. Geometry of the Dam and Reservoir Water

2. Kinta Rcc Dam and Galleries

The Kinta dam is the first Roller Compacted Concrete (RCC) dam which is located in Malaysia, in the province of Ipoh. The location of opening inside the Kinta RCC dam body is illustrated in Fig. 1 (Board of Engineers Malaysia (BEM), 2006).The shape and size of openings will vary in this study based on this figure.

Typical geometry of the Kinta RCC dam including reservoir water is elaborated in Fig. 2. In design of the large dams, the openings are not considered unless the maximum cross-sectional dimension of the gallery *'d'* is either ≥ 6 m or concrete cover anywhere around ≤ d (IS 12966-2, 1990).

In this case study, the selected size and shape of galleries is defined as Table 1. The different sizes of square, octagon and circle, defined in Table 1, are considered to evaluate the seismic analysis of the dam and can be categorized into following systems:

(a) Dam without gallery (System 1)
(b) Dam with small size gallery includes square and octagon shape (System 2)
(c) Dam with large size gallery includes circle, square and octagon shape (System 3)

The modeling of the above systems is carried out using finite element software, ABAQUS (version 6.10). This software is used for different nonlinear static and dynamic analysis such as water wave and seismic loadings (M.A. Lotfollahi Yaghin and Hesari, 2008).

Table 1. The Size and Shape of Openings

Gallery	Square	Square	Octagon	Octagon	Circle
Shape	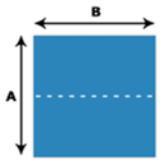	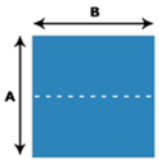	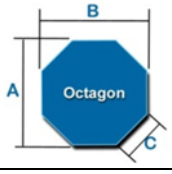	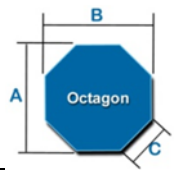	
Size(m)	A=2.5 B=2.5	A=6.5 B=6.5	A=2.5 B=2.5 C=1.18	A=6.5 B=6.5 C=3.06	D = 6.5

Table 2. Number of Nodes and Elements for Finite Element Discretization

Block	No. of Nodes	No. of Elements
Dam Without Gallery	609	560
Dam with Small Square Shaped	747	677
Dam with Large Square Shaped	778	694
Dam with Small Octagon Shaped	898	820
Dam with Large Octagon Shaped	900	825
Dam with Large Circle Shaped	1182	1095
Reservoir Water	551	504

3. Finite Element modeling of the Dam and Reservoir

A typical section of the Kinta RCC dam with the reservoir has been shown in Fig. 2. The number of nodes and elements for modeling of the systems with different size and shape of the galleries are given in Table 2.

A piece of the deepest section is used for finite element discretization. The specified elements for discretization of the dam-reservoir are mentioned as below:

a) CPS4R: Four node bilinear plane stress quadrilateral finite elements, reduced integration and hourglass control to represent the dam body.

b) AC2D4: Four node linear two-dimensional acoustic quadrilateral finite elements to represent the reservoir water.

The finite element discretization of the dam section and reservoir is carried out as shown in Figs. 3 and 4 respectively. The mesh of the dam body is generated in such a way to simulate the construction phase. The RCC dams are made by concrete and it is defined as a composite material which undergoes major strain softening (J.G.M., 1997). FE modeling of this behavior of the concrete materials may engage the matter of mesh sensitivity. To solve this difficulty, many solutions have been offered. One of the solutions is Concrete Damaged Plasticity (CDP) model which provide a general capability for the analysis of concrete structures under cyclic and/or dynamic loading. The major failure mechanisms in the dam body are crushing in compression and cracking in tension. The brittle behavior of concrete vanishes while the limited pressure is sufficient to avoid crack propagation. In these conditions, failure is driven by the stabilization and collapse of the concrete microporous microstructure lead to a macroscopic response which resembles the ductile material with work hardening (Abaqus Inc., 2010).

4. Equation of the Coupled Dam-reservoir Interaction

The system of dam-reservoir acts as a couple system under seismic analysis, thus the equations below can be represented as a comprehensive equation of the dam-reservoir interaction which includes two differential equations of the second order (Ghaemian, 2000):

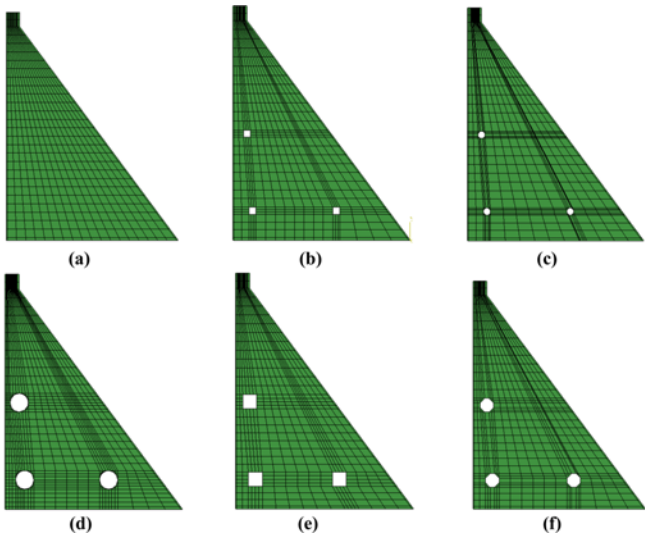

Fig. 3. Finite Element Discetization of Kinta Dam by Considering the Galleries: (a) No Gallery (b) Small Square (c) Small Octagon, (d) Large Circle, (e) Large Square, (f) Large Octagon

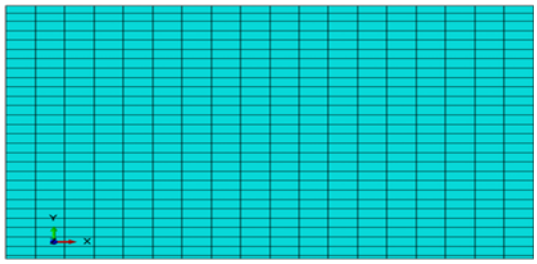

Fig. 4. Finite Element Discretization of the Reservoir Water

$$[M]\{\ddot{U}\}+[C]\{\dot{U}\}+[K]\{U\} = \{f_1\}-[M]\{\ddot{U}_g\}+[Q]\{p\} = \{F_1\}+[Q]\{p\} \quad (1)$$

$$[G]\{\ddot{p}\}+\{C'\}\{\dot{p}\}+[K']\{p\} = \{F\}-\rho[Q]^T(\{\ddot{U}\}+\{\ddot{U}\}_g) = \{F_2\}-\rho[Q]^T\{\ddot{U}\} \quad (2)$$

In Eq. (1) and (2), M, C and K represents mass, damping and stiffness of the dam and G, C' and K' are mass, damping and stiffness of reservoir water, respectively.The $[Q]$ is the coupling matrix, $\{f_1\}$ is the body force vector and hydrostatic force, $\{F\}$ is the force vector, $\{U\}$ and $\{p\}$ are the displacements and hydrodynamic pressures vectors. The $\{\ddot{U}_g\}$ is the earthquake acceleration and ρ is the water density of reservoir.The dot is representative of the time derivative.

5. Concrete Damaged Plasticity (CDP)

The linear assumption may not suitable for seismic analysis of the RCC dams (Zhang and Wang, 2013). In order to explain the complicated mechanical response of the concrete materials under seismic excitations, many constitutive approaches have been proposed including damage model, anisotropic damage and

isotropic damage model. A fundamental constitutive model proposed (Lubliner *et al*., 1989) and modified (J and GL, 1998). The method explaining the nonlinear behavior of each combinatorial material in a multiphase composite material is generally used in the cracking analysis for concrete dams. This model factorizes the uniaxial strength functions into two divisions to stand for the permanent degradation of stiffness and deformation. The model assumes two major failure mechanisms for concrete materials, the first for cracking and the second one for crushing in tension and compression, respectively.

In the incremental theory of plasticity the strain tensor (ε) is divided into two parts including the elastic strain (ε^e) and plastic strain (ε^p) in which for the linear elasticity can be written as:

$$\varepsilon = \varepsilon^e + \varepsilon^p \tag{3}$$

The variables $\{\varepsilon^e, \varepsilon^p, k\}$ are assumed to be identified at time (t). With mentioned information, for stress tensor the following can be obtained:

$$\sigma = (1-d)\bar{\sigma} = (1-d)E_0(\varepsilon - \varepsilon^p) \text{ and } d = d(k) \tag{4}$$

In which d is the scalar stiffness degradation variable which can be in the range of 0 (undamaged) to 1 (fully damaged); E_0 is the undamaged elastic stiffness for concrete material. The failure mechanism of the material associated with the damage, thus, reduction of the elastic stiffness that supposed a function of the internal variable $\{k\}$ including of the compressive and tensile variables, namely $k = (k_t, k_c)$. Function of damages consisting tension (d_t) and compression (d_c) which are nonlinear functions computed by uniaxial response in compression with practical data. Hence, the effective stress is determined as:

$$\bar{\sigma} = \frac{\sigma}{1-d} = E_0(\varepsilon - \varepsilon^p) \tag{5}$$

6. Material Propertiesand Loading Parameters

Three different types of materials are considered in the nonlinear dynamic analysis for the RCC dam body, CVC facing and CVC foundation. The isotropic material properties of the model in the nonlinear analysis are demonstrated in Table 3 (GHD, 2002).

The necessary parameters of the reservoir water includes Bulk modulus (K) and mass density which is considered as 2107 MPa (ρ_w) and 1000 kg/m^{3}respectively.

Table 3. Material Properties of the Dam

Material properties	RCC	CVC-Facing	CVC-Foundation
Young modulus (N/m^2)	0.23E+11	0.32E+11	0.23E+11
Poisson ratio v	0.2	0.2	0.2
Mass density ρ	2386	2352	2325
Compressive strength (Mpa)	20	40	20
Tensile strength (Mpa)	2	4	2
Dynamic Tensile strength (Mpa)	2.5	5	2.5
Allowable tensile strength (Mpa)	3.2	6.25	3.2

6.1 Hydrodynamic Pressure

In general, the reservoir hydrodynamic pressure in the preserved water is governed by the 2-D wave equation which is subjected to boundary conditions at: (1) the absorptive reservoir bottom (2) The free surface of the reservoir and (3) the upstream side of the dam (Fenves and Chopra, 1983). In this paper, the hydrodynamic pressure is modeled and subjected to aforementioned boundary conditions by means of the modeled water in the finite element software to assess the actual behavior of the dam under nonlinear time history analysis.

6.2 Seismic Loading

The Kinta RCC dam has been subjected to the transverse and vertical acceleration of the Koyna earthquake occurred in India on December, 1967, as plotted in Fig. 5(a) and (b) (Omidi et al, 2013) as well as response spectra (Fig. 5(c)). Therefore, in order to investigate the effect of earthquake accelerations on the dam, the transverse and vertical components are applied at the base of the dam and nonlinear time history seismic analysis has been carried out.

Damping is extraordinarily vital in dynamic analysis of dams to reproduce factual behaviors. In present study the nonlinear seismic analysis is conducted deliberating the damping of 5%. As a result, the natural frequencies ω_1 and ω_2 with values of 9.571 and 51.238 rad/sec is obtained according to the first and last modes of vibrations. This approach leads the values to be α = 0.806 and β = 0.00164 (Chopra, 2001). The α and β values are considered for nonlinear dynamic analysis.

7. Results and Discussions

The dam-reservoir has been subjected to the Koyna earthquake

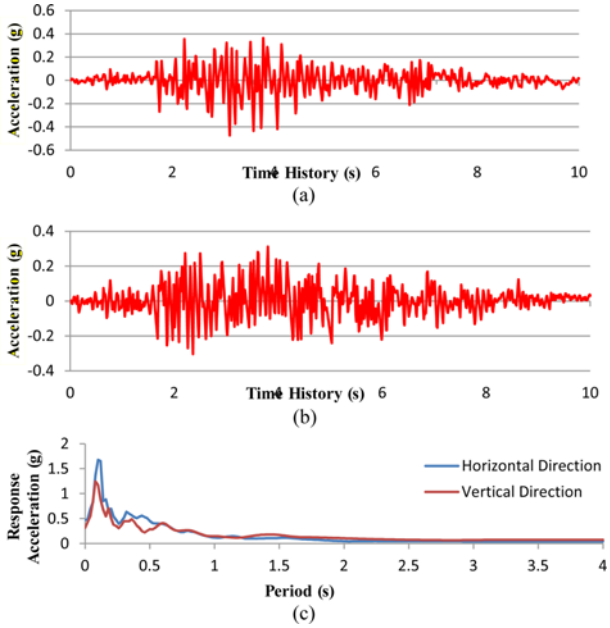

Fig. 5. Components of the Koyna Excitations: (a) Transverse Acceleration, (b) Vertical Acceleration, (c) Response Spectra

by considering of the galleries effects on the dam in three systems under nonlinear dynamic analysis. The topmost node (crest node) of the dam at upstream face is selected to consider horizontal displacement of the RCC dam body with considering different size and shape of the galleries, given in Table 1. The location of said node is shown in Fig. 2 too.

7.1 Displacement Analysis

The horizontal time history displacement in case of without gallery (system 1) and under different size of the small galleries (system 2) of the dam crest is plotted in Fig. 6.

From Fig. 6, it can be seen that, the gallery with square shape has less displacement in comparison to octagon shape for system 2. The maximum displacements values from Fig. 6 are found to be 2.88 cm and 3.18 cm for small square and small octagon shaped respectively. Also from this figure it can be seen that the gallery sizes have a significant direct effect on the dam in related to the displacement of the dam crest. The displacement value has been increased by approximately 80% from 2.88 cm to 5.2 cm for the small square and large square shaped. This amount is also observable for small and large octagon shaped, which has been increased by about 38% from 3.18 cm to 4.4 cm. Thus, when the size of galleries is increase, the displacements of the dam crest also increases. To investigate the effect of different shape of gallery on displacement values of the dam crest, three large galleries (system 3) including circle, square and octagon shaped are selected from Table 1. Based on above figure, it can found that the Kinta RCC dam with large circle shape has 4.17 cm displacement at the crest. However by changing the shape of the gallery to square and octagon, this amount varies to 5.2 cm and 4.4 cm respectively. These results show that the shape of the gallery also affect the dam crest displacement under seismic loadings.

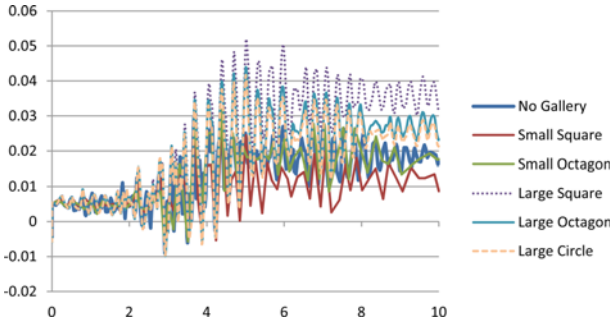

Fig. 6. Comparison of the Relative Horizontal Displacement at Dam Crest

Table 4 indicates the peak relative horizontal and vertical displacements of the Kinta RCC dam under earthquake excitation for effects of openings.

7.2 Stress Analysis

The maximum and minimum principal stress of the dam has to be carefully investigated. In particular, when the size and shape effects of

Table 4. Peak Horizontal Displacement of the Dam by Considering Gallery Effect

System		1	2		3		
		No Gallery	Square	Octagon	Circle	Square	Octagon
Dis. (cm)	Hor.	3.15	2.86	3.18	4.17	5.20	4.40
	Ver.	1.17	0.85	1.19	1.61	2.22	1.75

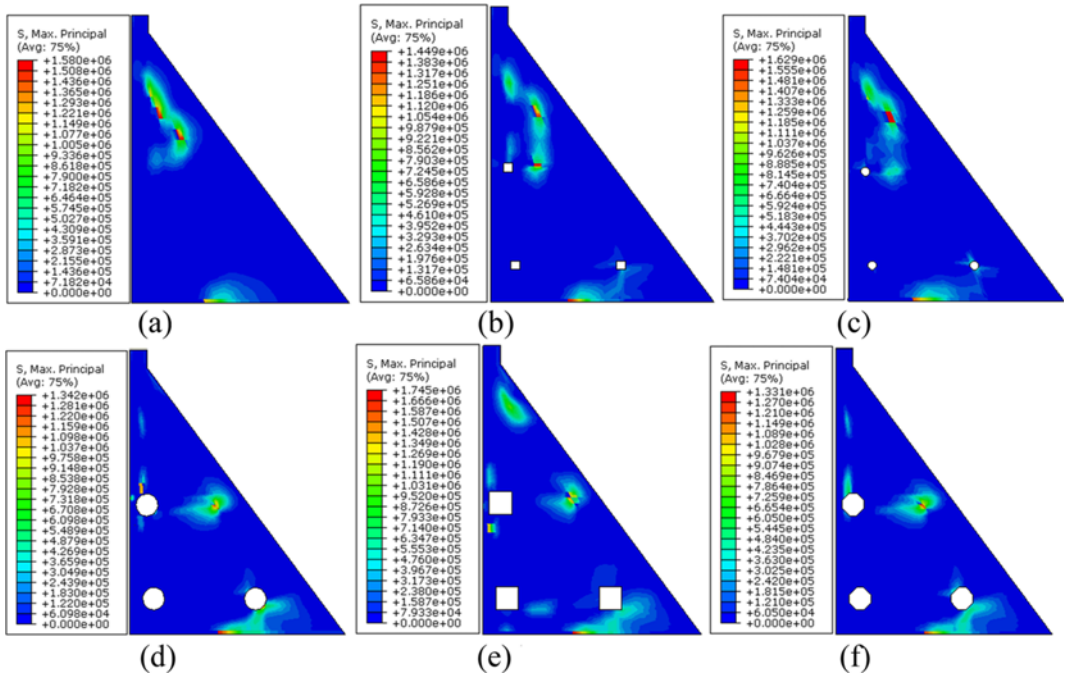

Fig. 7. Maximum Principal Stresses in Dam with and without Gallery: (a) No Gallery, (b) Small Square, (c) Small Octagon, (d) Large Circle, (e) Large Square, (f) Large Octagon

the openings are taken into account, these stresses are significantly visible on the dam and must be specifically inspected.

7.2.1 Stress Distribution around Galleries

The stresses in whole RCC dam body are also investigated by means of contour lines. Fig. 7 displays the distribution of the maximum principal stresses for entire RCC dam body under earthquake excitation by taking water hydrodynamic pressure into account. From Fig. 7, it can be observed that the stresses around large openings are tangible compared with small openings and without opening. Also, the distribution of the maximum principal stresses around large openings shows that in the square shaped the stresses are lesser than circle and octagon shaped especially around top openings and right side openings for system 3. These descriptions are indicated in part (d), (e) and (f).

The gallery effects in case of the minimum principal stresses on the Kinta RCC dam under seismic loading are depicted in contour lines in Fig. 8. The minimum stress value for dam without gallery is -3.014 Mpa. This amount is decreased in system 2 with existence of two small square and octagon shaped to -3.321 Mpa and -3.524 Mpa respectively. While the size of galleries is increased, the aforesaid values are rapidly reduced to -8.144 Mpa, -6.355 Mpa and -5.127 Mpa for circle, square and octagon shaped by 170%, 111% and 70% respectively. However, the stresses around gallery with circle shape has lesser compared to two other cases in system 3 as shown in Fig. 8(d) given by colors in contour lines.

7.2.2 Stress Concentrations around Galleries

Time history analysis of maximum and minimum stresses around galleries is illustrated in Fig. 9 for system 2 and 3 under Koyna earthquake. As depicted in this figure, stress around galleries increases when large galleries are taken into account in system 3. In addition, amongst three different shapes of galleries in system 3, it can be concluded that the gallery with octagon and square shapes have highest stress values around themselves.

7.3 Tensile Damage and Crack Pattern in RCC Dam Body

Based on the uniqueness of the cracking development in various dams, the damage propagation of the Kinta RCC dam is inspected in different conditions with and without effect of galleries. The starting point of the cracking is formed from the lowest element at heel region in upstream face and it propagates toward downstream side. By reaching to the peak acceleration of

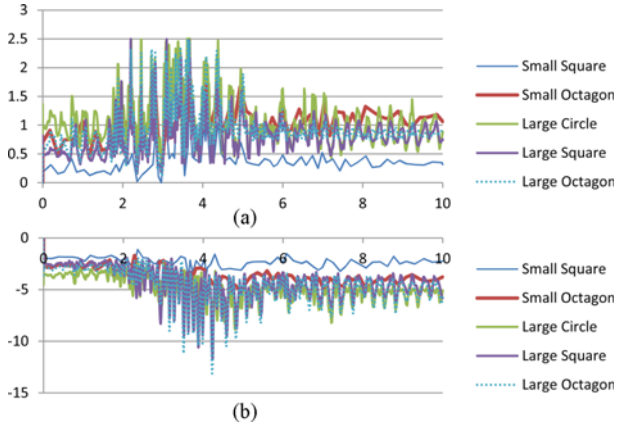

Fig. 9. Stress Concentration around the Galleries under Koyna Excitations: (a) Maximum Stress, (b) Minimum Stress

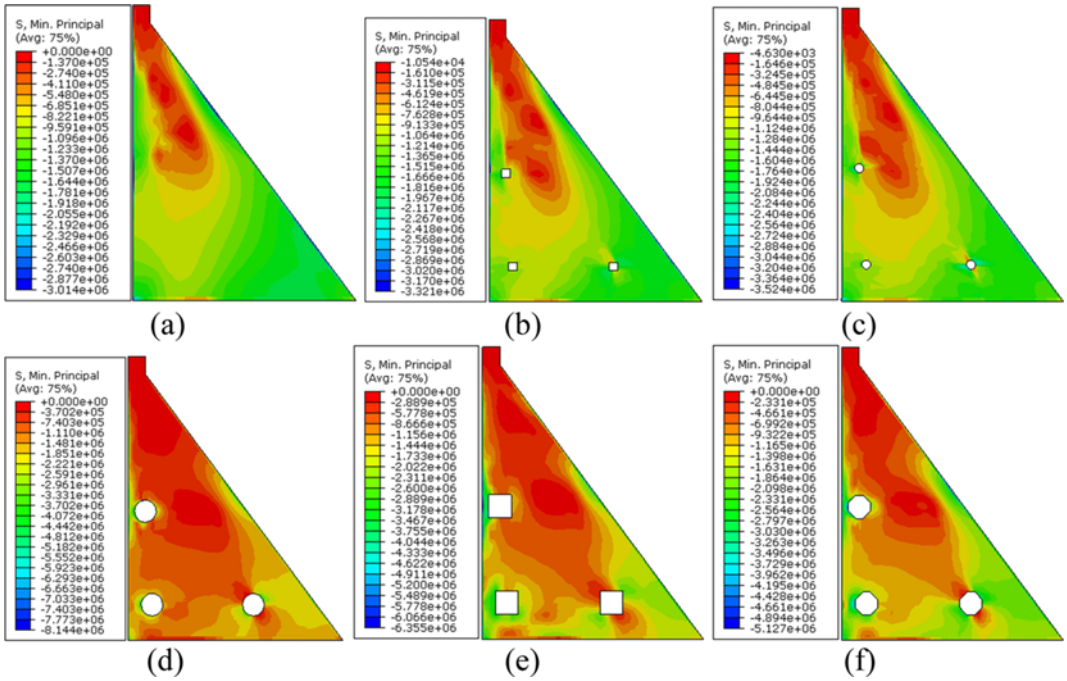

Fig. 8. Minimum Principal Stresses in Dam with and without Gallery: (a) No Gallery, (b) Small Square, (c) Small Octagon, (d) Large Circle, (e) Large Square, (f) Large Octagon

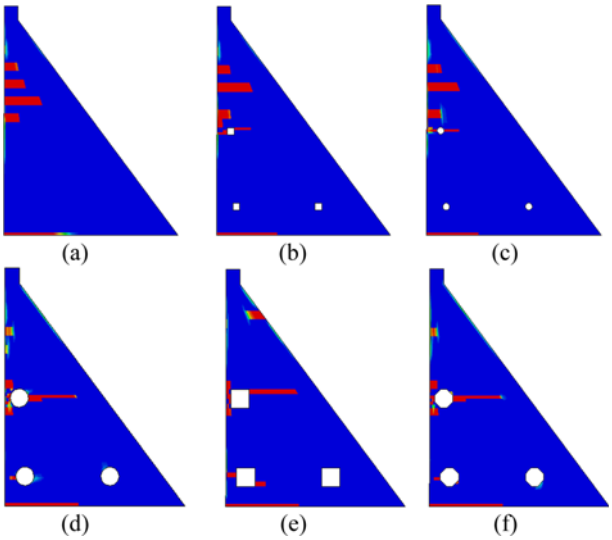

Fig. 10. Tensile Damage Response of the Dam with and without Gallery: (a) No Gallery, (b) Small Square, (c) Small Octagon, (d) Large Circle, (e) Large Square, (f) Large Octagon

the Koyna earthquake and by considering the effect of hydrodynamic pressure due to the reservoir water, the middle zone of the RCC dam in upstream face absorbs some damages as well. The tensile damage response of the dam with and without gallery is shown in Fig. 10.

With considering small galleries, the cracking pattern is varied and the dam is suffered at the place of openings too. This phenomenon is determined in part (b) and (c). By enlarging the size of galleries, the crack propagations are expanded to verge of the downstream face. In general, when the cracking starts its propagation from upstream face, this opens pores to water flow and cause damage of the dam. In system 3, the cracking around circle shaped and octagon shaped is observed more than square shaped in upstream face especially in place of the upper galleries in three cases as illustrated in part (d), (e) and (f). This event is dependent on the tensile stresses of the dam due to the hydrodynamic pressure and galleries shape under dynamic analysis.

8. Generalization

To generalize the results of the nonlinear dynamic analysis of the Kinta RCC dam under Koyna earthquake, two more earthquake excitations are considered and the outcomes are plotted in below figures. For this aim, the excitations of the Altadena and Petrolia are applied to the dam. The results are given in terms of the crest displacement, stress concentration around galleries and the crack propagations. Fig. 11 shows the component of two mentioned earthquakes.

8.1 Displacement Analysis

Time history horizontal displacements of the dam crest for the dam models under two mentioned earthquake excitations are

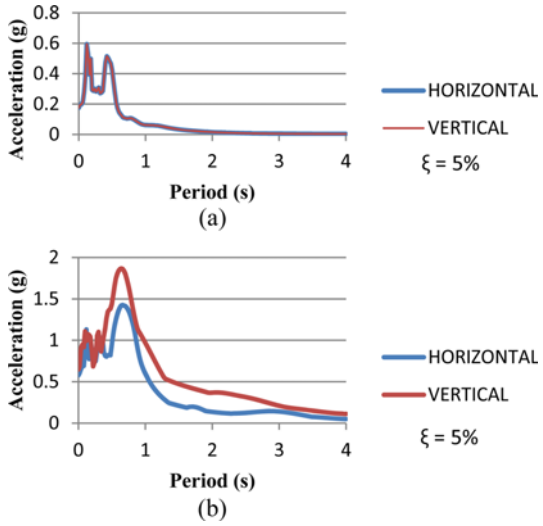

Fig. 11. Response Spectra of: (a) Altadena and (b) Petrolia Earthquakes

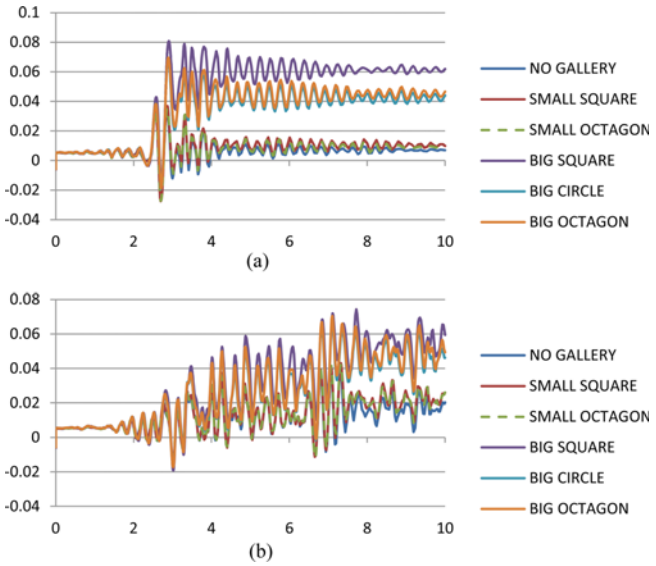

Fig. 12. Time History Displacement Response of the Dam under Selected Motions: (a) Altadena, (b) Petrolia

separately shown in Fig. 12.

From Fig. 12(a) it can be observed that, the maximum horizontal displacement of dam crest for dam without gallery is 3.42 cm in downstream direction. For system 2, there is 7.6% and 3% increase of displacement with 3.68 cm and 3.52 cm for small square and small octagon gallery respectively. These percentages of difference for system 2 relative to system 1 can be neglected. However, the percentages of variations for system 3 compared to system 1 are remarkable and have to be taken into account. Presence of large gallery inside the dam body causes the crest displacement of 8.1 cm, 6.81 cm and 6.95 cm for dam with large square, circle and octagon shape respectively. These amounts gives 137%, 99% and 103% difference compare to the case when no gallery is considered. By comparing the displacement values in system 3, it is found that the dam with large circle has

Table 5. Peak horizontal Displacement (cm) of the Dam Considering Gallery Effect

System	1	2		3		
	No Gallery	Square	Octagon	Square	Circle	Octagon
Altadena Response	3.42	3.68	3.52	8.1	6.81	6.95
Petrolia Response	3.89	4.31	4.23	7.43	6.81	7.03

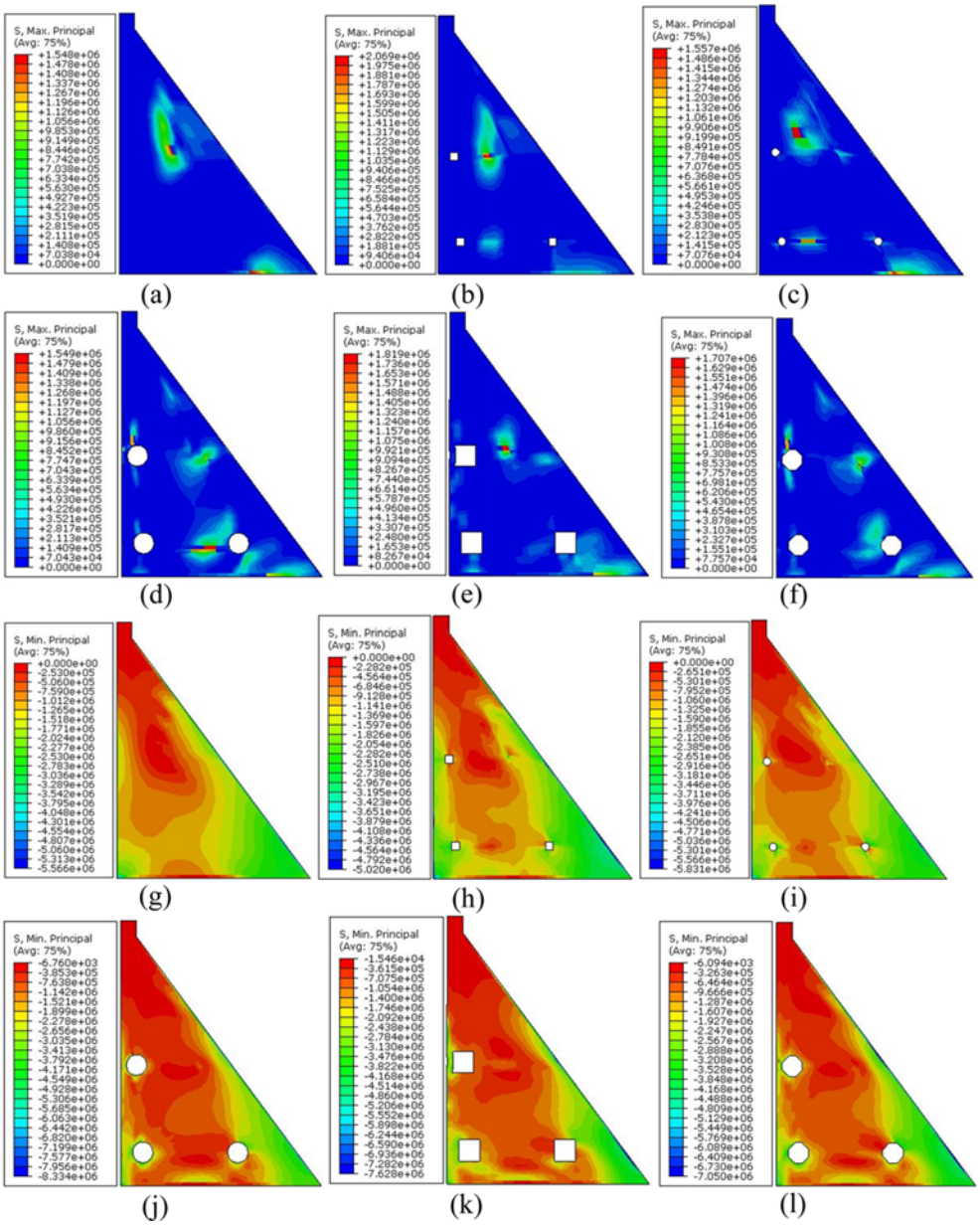

Fig. 13. Maximum and Minimum Principal Stresses in Dam with and without Gallery under Altadena Excitations: (a) No Gallery, (b) Small Square, (c) Small Octagon, (d) Large Circle, (e) Large Square, (f) Large Octagon, (g) No Gallery, (h) Small Square, (i) Small Octagon, (j) Large Circle, (k) Large Square, (l) Large Octagon

minimum displacement relative to large square and octagon shape. In contrast, existence of the large square causes maximum displacement.

From Fig. 12(b) similar results can be obtained for Petrolia earthquake in terms of displacement response. Considering behavior of the Kinta RCC dam under Petrolia excitations illustrates again that, the maximum displacements of the dam crest in system 2 and 3 belong to the gallery with square shape. In system 2 the displacement of the dam crest with square shape is 4.31 cm. This value gives approximately 11% increase of displacement compared with system 1 by 3.89 cm movement in positive (downstream) direction. Likewise, a difference of 91%

for crest displacement occurred compared to system 1, when the dam with large square is considered. In contrast, the minimum crest displacement in system 3 is experienced by the dam with circle shape (6.82 cm), whereas, this amount is 7.03 cm for the dam with octagon shape. The tabular values of the dam crest displacement are shown in Table 5 for two different aforesaid earthquakes motions.

8.2 Stress Distribution around Galleries

The stress distribution contours in three different systems under two different earthquakes are shown in Fig. 13 and 14. The maximum stress developments of the dam body are demonstrated in Fig. 13(a) to 13(f). The contour lines show that, when small and large galleries are taken into account, the position and values of maximum stresses vary compared to the dam without gallery. In addition, existence of the gallery causes stress around galleries. In system 2 and 3, the maximum stresses are experienced by the dam with presence of square shaped gallery with value of 2.07 Mpa and 1.81 Mpa and it increases by 34.4% and 17.5% respectively, compared to the dam without gallery. Also, Fig. 13(g) to 13(l) indicates the minimum stresses. Consideration of the gallery effects shows that the circle shape has less stress concentration around the gallery in comparison to square and octagon shapes in system 3. The maximum stress is absorbed by

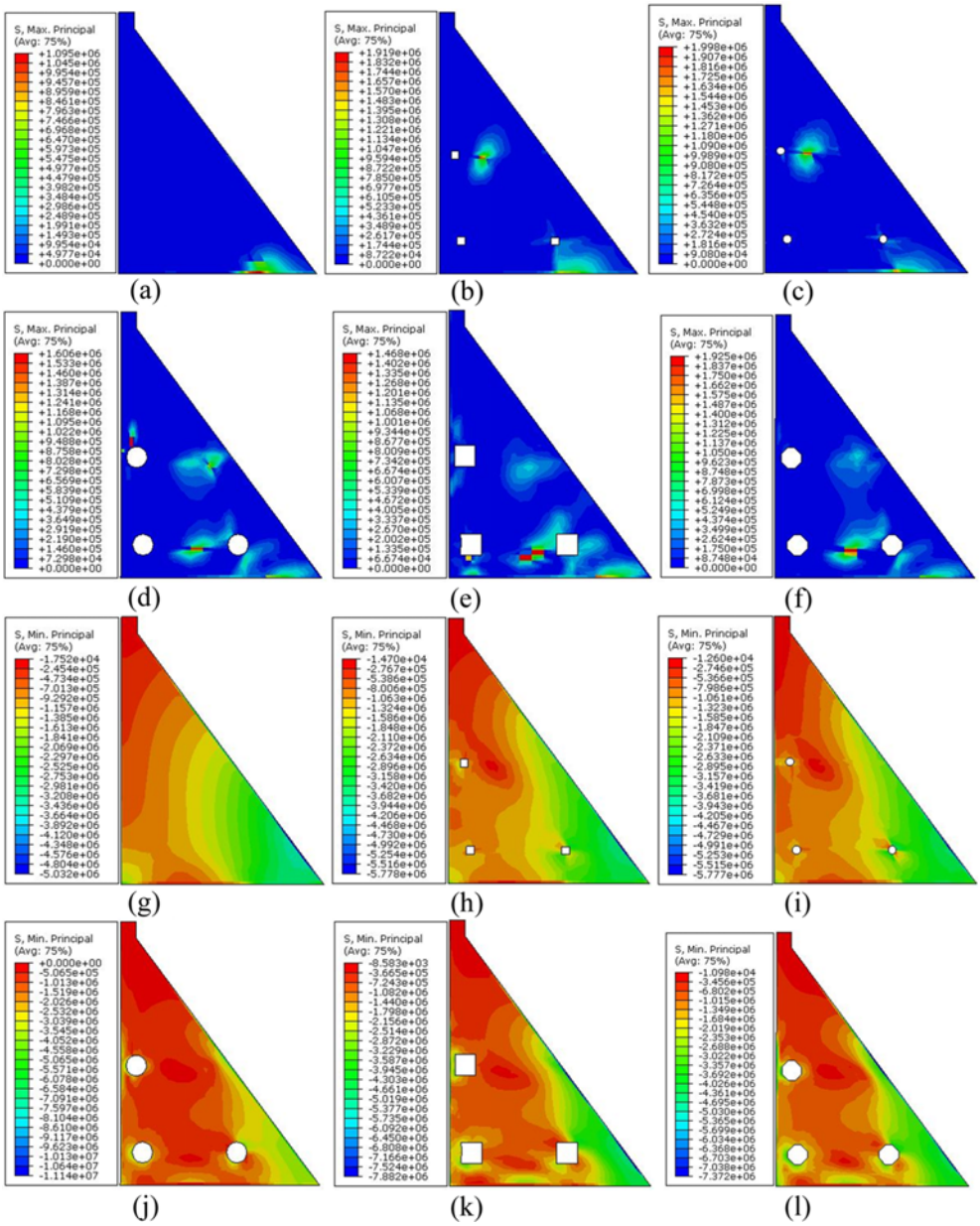

Fig. 14. Maximum and Minimum Principal Stresses in Dam with and without Gallery under Petrolia Excitations: (a) No Gallery, (b) Small Square, (c) Small Octagon, (d) Large Circle, (e) Large Square, (f) Large Octagon, (g) No Gallery, (h) Small Square, (i) Small Octagon, (j) Large Circle, (k) Large Square, (l) Large Octagon

gallery with square shape.

Figure 14(a) to 14(f) show the maximum principal stresses. Again, the presence of galleries proves that the stresses are dragged toward galleries. As shown in Fig. 14(e), the most stress distribution is occurred around gallery with square shape at the bottom zones compared to the galleries with circle and octagon shape. This phenomenon can also be observed for minimum principal stresses given in Fig. 14(g) to 14(l). Considering the dam in these figures for small galleries in system 2, shows more stress concentration around square shaped gallery compared to octagon shape. The presence of large gallery encourages this consequence. The value of the minimum stress for dam with square shape and octagon shape is -7.88 Mpa and -7.37 Mpa. These values show a difference of 56.7% and 46.5% relative to the dam without gallery with minimum stress value of -5.03 Mpa. Conversely, the dam experiences less stresses around the circle shape in comparison to other cases in system 3.

8.3 Stress Concentrations around Galleries

Inspection of maximum and minimum stress time histories around galleries for system 2 and system 3 are shown in Fig. 15 and 16 under Altadena and Petrolia earthquakes respectively. The size and shape effects of the galleries can clearly noticed in these figures. Increase in gallery size in system 3, causes significant stresses around them in compare to system 2. The galleries with various shapes have different responses and behavior in case of stress attraction around galleries in system 2 and 3. However, the maximum and minimum stress concentration values around galleries are almost near to each other in system 3. Investigation of the shape effect under general responses during time history analysis shows that galleries with octagon and square shapes attract highest stresses around themselves in most cases.

8.4 Tensile Damage and Crack Pattern in RCC Dam Body

Figure 17 depicts the crack pattern under Altadena excitations.

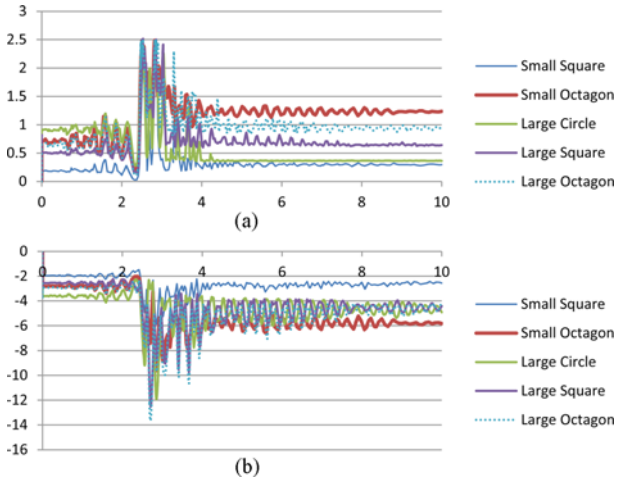

Fig. 15. Stress Concentration around the Galleries under Altadena Excitations: (a) Maximum Stress, (b) Minimum Stress

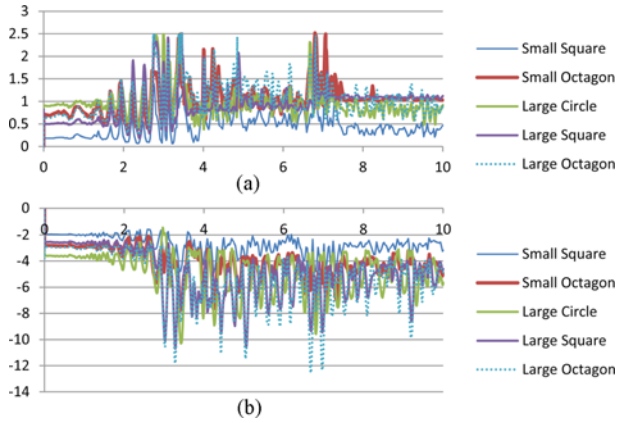

Fig. 16. Stress Concentration around the Galleries under Petrolia Excitations: (a) Maximum Stress, (b) Minimum Stress

As shown in Fig. 17(a), cracks appeared at the heel and downstream zones for the dam without gallery. However, the dam with small square and octagon shape (Fig. 17(b) and Fig. 17(c)) experiences cracks almost at same locations, but it suffers some damages around the left bottom openings for both cases in system 2. From Fig. 17(d) to Fig. 17(f) the effect of large galleries is apparent, where the location of cracks is totally changed with more intensity at upstream face. Amongst various shape of galleries in system 3, although, it seems that the dam with circle and octagon shape have less level of damage, but considering the right bottom gallery in both condition, shows less cracking for circle form compared to the octagon shape. Fig. 17(e) illustrates severity of damage level of dam with large square shape gallery.

The damage responses of the Kinta RCC dam under Petrolia

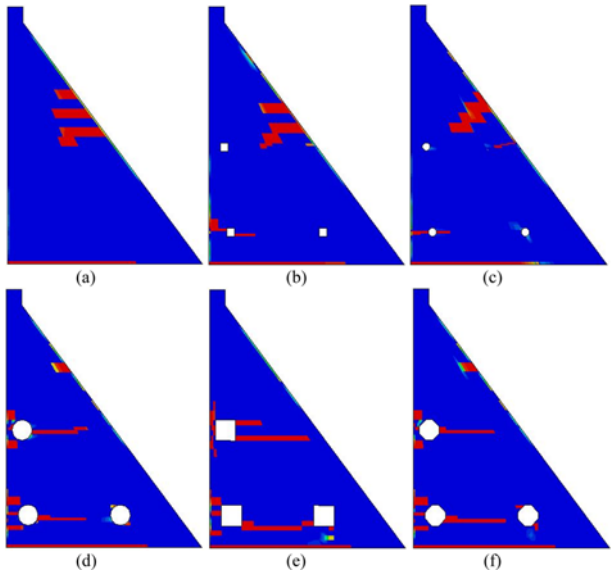

Fig. 17. Tensile Damage Response of the Dam with and without Gallery under Altadena Earthquake: (a) No Gallery, (b) Small Square, (c) Small Octagon, (d) Large Circle, (e) Large Square, (f) Large Octagon

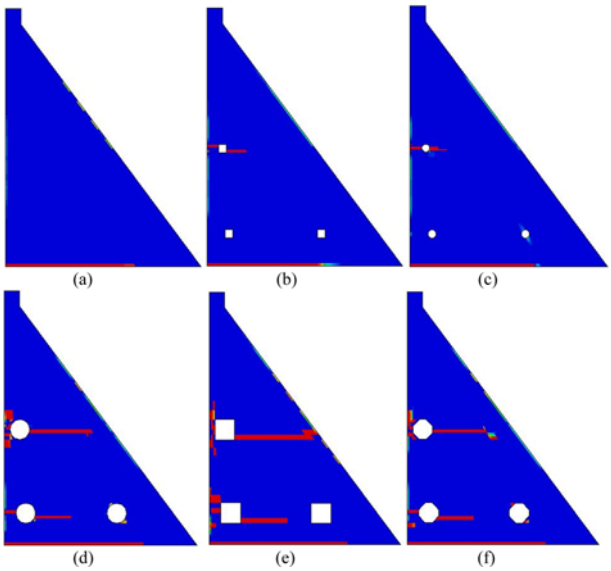

Fig. 18. Tensile Damage Response of the Dam with and without Gallery under Petrolia Earthquake: (a) No Gallery, (b) Small Square, (c) Small Octagon, (d) Large Circle, (e) Large Square, (f) Large Octagon

excitations are demonstrated in Fig. 18. Comparison of the different shape and size of galleries shows the noticeable effect of galleries. From Fig. 18(b) and Fig. 18(c) the crack propagation of the middle area at the upstream side caused by galleries is observable, whereas, the dam without gallery has no crack in this region. Fig. 18(d) to Fig. 18(f) shows the intensity of crack for the dam with circle, square and octagon shapes. As illustrated in figures, the maximum and the minimum cracking is occurred for square and circle shapes respectively.

9. Conclusions

The nonlinear time history displacement, stress analysis and damage response of the Kinta RCC dam has been inspected by considering the effect of galleries divided into three systems on the basis of different sizes and shapes. The hydrodynamic pressure due to reservoir water has been imposed to the dam. For this purpose, 2-D finite element discretization has been performed by means of finite element software, ABAQUS. To generalize the conclusions, two more earthquakes are applied to the dam. From the obtained results, following points are drawn:

1. Displacements of the dam crest with existence of large galleries (system 3) are 65%-80% larger than that with small galleries (system 2) and without gallery (system 1) under Koyna earthquake. Crest displacement under Altadena and Petrolia earthquakes increases by 120%-137% and 72%-91% respectively.
2. Presence of galleries changes the position of maximum stress contours. It attracts the stresses around galleries.
3. Minimum principal stresses of the dam heel zone in system 3 are approximately 19%, 48%, 100% and 25% higher than system 1and about 37%, 43%, 75% and 13% more than stresses in system 2 under Koyna, Altadena, Petrolia and Pomona earthquake respectively.
4. Generalization of the results indicates that the dam with large circular gallery has minimum stresses around the gallery in comparison to the dam with large square and octagon shape in system 3.
5. Minimum stress distributions inside the dam body are significantly increased when the large openings are taken into account.
6. Cracking pattern and its propagations is changed when the small and large galleries are considered in the analysis.
7. Based on the damage response, the circular gallery experiences lesser damage around itself compared to other two cases in system 3.

In general, from above discussions it can be concluded that the top displacement is significantly affected by the area of gallery and by the location of the gallery. When the area of the gallery is small, its shape is not significant for the displacement. Therefore, the dam with circle shaped gallery behaves better than square and octagon shape gallery in relation to crack propagations, displacements and stress concentration around gallery. Conversely, in case of the displacement response, gallery with large square and octagon shape had maximum displacement and the most stresses around galleries are attracted by square shape.

Acknowledgements

The authors gratefully acknowledge the supported given by University Malaya Research Grant (UMRG-Project No. RP004A/13AET) and Fundamental Research Grant Scheme, Ministry of Education, Malaysia (FRGS-Project No. FP028/2013A).

References

Abaqus Inc. (2010). *Abaqus theory manual*, Version 6.10. Abaqus Inc. (n.d.).

Aguíñiga, F., Jaiswal, M., Sai, J. O., Cox, D. T., Gupta, R., and van de Lindt, J. W. (2010). *Experimental study of tsunami forces on structures*, Vol. 361, pp. 111-118.

Ahmad, S. M. (2007). *Design of waterfront retaining wall for the passive case under earthquake and tsunami*.

Akkose, M., Bayraktar, A., and Dumanoglu, A. A. (2008). "Reservoir water level effects on nonlinear dynamic response of arch dams." *Journal of Fluids and Structures*, Vol. 24, No. 3, pp. 418-435.

Akköse, M. and Şimşk, E. (2010). "Non-linear seismic response of concrete gravity dams to near-fault ground motions including dam-water-sediment-foundation interaction." *Applied Mathematical Modelling*, Vol. 34, No. 11, pp. 3685-3700.

Arash Mazloumi, Ghaemian, M. and Noorzad, A. (2012). *Nonlinear seismic analysis of rcc dam considering orthotropic behavior of layers*, In International Symposium On Dams For a Changing World.

Ayari, M. L. (1990). "A fracture mechanics based seismic analysis of concrete gravity dams using discrete cracks." *Engineering Fracture Mechanics*, Vol. 35, Nos. 1/2/3, pp. 587-598.

Board of Engineers Malaysia (BEM) (2006). Engineering Practice.

Bower, A. F. (2010). *Applied mechanics of solids*, (Taylor & Francis Group, Eds.). Boca Raton: CRC Press.

Calayir, Y. and Karaton, M. (2005). "Seismic fracture analysis of concrete gravity dams including dam–reservoir interaction." *Computers & Structures*, Vol. 83, Nos. 19-20, pp. 1595-1606.

Chopra, A. K. (2001). *Dynamics of structures theory and applications to earthquake engineering*, New Jersey: Prentice-Hall.

Fenves, G. and Chopra, A. K. (1983). "Effects of reservoir bottom absorption on earthquake response of concrete gravity dams." *Earthquake Engineering and Structural Dynamics*, Vol. 11, No. 6, pp. 809-829.

Ghaemian, M. (2000). *Concrete dams: Seismic analysis, Design and Retrifitting*.

GHD (2002). *Study of restrictions on RCC temperature,* Stage 2 development of Ipoh water supply.

Guanglun, W., Pekau, O. A., Chuhan, Z., and Shaomin, W. (2000). *Seismic fracture analysis of concrete gravity dams based on nonlinear fracture mechanics*, Engineering Fracture Mechanics, 65.

IS 12966-2 (1990). *Code of practice for galleries and other openings in dams,* Part 2: Structural Design [WRD 9: Dams and Spillways]. India.

J, L. and GL, F. (1998). "Plastic-damage model for cyclic loading of concrete structures." *Journal of Engineering Mechanics*, Vol. 124, No. 8, pp. 892-900.

J. G. M. van Mier (1997). *Fracture process of concrete: Assessment of material parameters for fracture models*, Boca Raton, Florida: CRC Press, Inc.

Jiang, S. and Du, C. (2012). *Seismic stability analysis of concrete gravity dams with penetrated cracks*, Vol. 5, No. 2007, pp. 105-119.

Jin, C., Soltani, M., and An, X. (2005). "Experimental and numerical study of cracking behavior of openings in concrete dams." *Computers & Structures*, Vol. 83, Nos. 8-9, pp. 525-535.

Long, Y., Zhang, C., and Xu, Y. (2009). "Nonlinear seismic analyses of a high gravity dam with and without the presence of reinforcement." *Engineering Structures*, Vol. 31, No. 10, pp. 2486-2494.

Lubliner, J., Oliver, J., Oller, S., and Oñate, E. (1989). "A plastic-damage model for concrete." *International Journal of Solids and Structures*, Vol. 25, No. 3, pp. 299-326.

M. A. Lotfollahi Yaghin and Hesari. (2008). "Dynamic analysis of the arch dam under earthquake force with ABAQUS." *Journal of Applied Sciences*, Vol. 8, No. 15, pp. 2648-2658.

Omidi, O., Valliappan, S., and Lotfi, V. (2013). "Seismic cracking of concrete gravity dams by plastic–damage model using different damping mechanisms." *Finite Elements in Analysis and Design*, Vol. 63, pp. 80-97.

Paggi, M., Ferro, G., and Braga, F. (2013). "A multiscale approach for the seismic analysis of concrete gravity dams." *Computers & Structures*, Vol. 122, pp. 230-238.

Perumalswami, P. R. and Kar, L. (1973). "Earthquake behavior of arch dams-reservoir systems." *Fifth World Conference on Earthquake Engineering*, Rome, Italy.

Shirkande, A. S. (2011). "3 D Stress analysis around large openings in concrete gravity dam." *International Journal of Earth Sciences and Engineering*, Vol. 4, No. 6, pp. 600-603.

Skrikerud, P. and Bachmann, H. (1986). "Discrete crack modeling for dynamically loaded, unreinforced concrete structures." *Earthquake Engineering & Structural Dynamics*, Vol. 14, No. 2, pp. 297-315. 17.

Zhang, S. and Wang, G. (2013). "Effects of near-fault and far-fault ground motions on nonlinear dynamic response and seismic damage of concrete gravity dams." *Soil Dynamics and Earthquake Engineering*, Vol. 53, pp. 217-229.

Zhang, S., Wang, G., and Yu, X. (2013). "Seismic cracking analysis of concrete gravity dams with initial cracks using the extended finite element method." *Engineering Structures*, Vol. 56, pp. 528-543.

Zhu, X. and Pekau, O. A. (2007). "Seismic behavior of concrete gravity dams with penetrated cracks and equivalent impact damping." *Engineering Structures*, Vol. 29, No. 3, pp. 336-345.